Supplementary Materials for

Lung tumoroids as a testing platform for precision CAR T-cell therapy

Lukas Ehlen & Martí Farrera-Sal *et al.*

Corresponding author. Michael Schmueck-Henneresse, Email: michael.schmueck-henneresse@bih-charite.de

This PDF file includes:

Extended Data Figures S1 to S10

Extended Data Fig.1: Establishment of lung tumoroids and healthy organoids and correlation with clinical data.

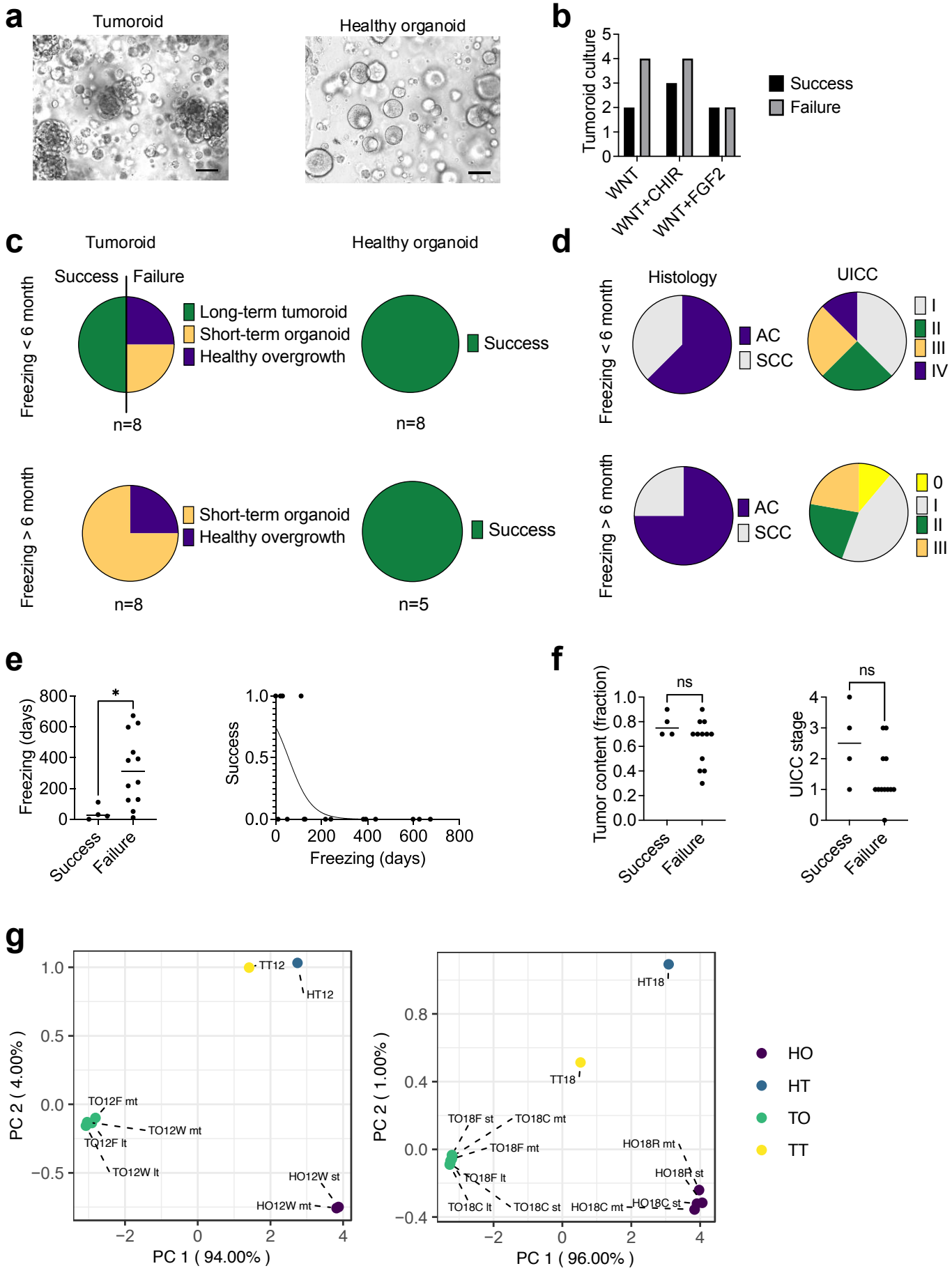

Extended Data Figure 1. Establishment of lung tumoroids and healthy organoids and correlation with clinical data. a, Brightfield images of matched tumoroids (TO) and healthy organoids (HO). Scale bar, 100 µm. **b,** Success and failure of tumoroid cultures using different growth factor cocktails: Basal medium (BM) + RSPO1, Noggin, FGF7/FGF10, WNT (WNT); BM + RSPO1, Noggin, FGF7/FGF10, WNT, CHIR (WNT+CHIR); BM + RSPO1, Noggin, FGF2, WNT (WNT+FGF2). **c**, Success and failure rates of TO and HO from tissues frozen for less than or more than 6 months (see Supplementary Table 1 for freezing duration details). "N" indicates number of patients from whom TO and HO were derived. The establishment of long-term tumoroids (growth > 6 months, maintaining tumor genomic identity) or healthy organoids (growth > 3 months) is shown in purple. Short-term organoid cultures (growth < 6 months) are in yellow, and overgrowth of tumor cells by healthy organoids (based on DNA sequencing) is in green. **d**, Selected patient characteristics from (tumor-) tissues with varying freezing durations. Left: Histological subtype, with adenocarcinoma (AC) shown in purple and squamous cell carcinoma (SCC) in grey. Right: UICC clinical stage of the patients. For detailed clinical data, refer to Supplementary Table 1. **e**, Left: Mann-Whitney test comparing successful (n=4) and failed (n=12) tumoroid cultures. "Success" and "failure" are patient-specific, as multiple tumoroid cultures per patient were tested with different growth factor combinations. Mean freezing days (FD): 40.5 in the success group vs. 323 in the failure group. Rank sum: 14 (success group) vs. 122 (failure group). Two-tailed P value = 0.0132. Right: Simple logistic regression model evaluating the relationship between success rate and freezing duration. Tjur's R^2 goodness-of-fit: 0.4321. Example predicted success rates: 0 FD = 0.752; 15 FD = 0.69; 30 FD = 0.621; 60 FD = 0.477; 90 FD = 0.337. **f,** Mann-Whitney test comparing tumor content in primary tumors (tumor cells/all cells in tumor specimens) and UICC disease stage in patients with successful vs. failed tumoroid cultures. Mean tumor content: 0.775 (success group) vs. 0.633 (failure group). Mean UICC stage: 2.5 (success group) vs. 1.417 (failure group). **g,** Principal component analysis (PCA) of DNA methylation levels in patient 12 and patient 18 for TT, HT, TO, and HO samples. Short-term (st), mid-term (mt), and long-term (lt) organoid cultures are included. R = RSPO culture medium, C = WNT+CHIR culture medium, F = WNT+FGF2 culture medium.

Extended Data Fig.2: Continuation of Lung tumoroids preserve the histological and proteome landscape of their parental tumors and enable individualized proteome profiling.

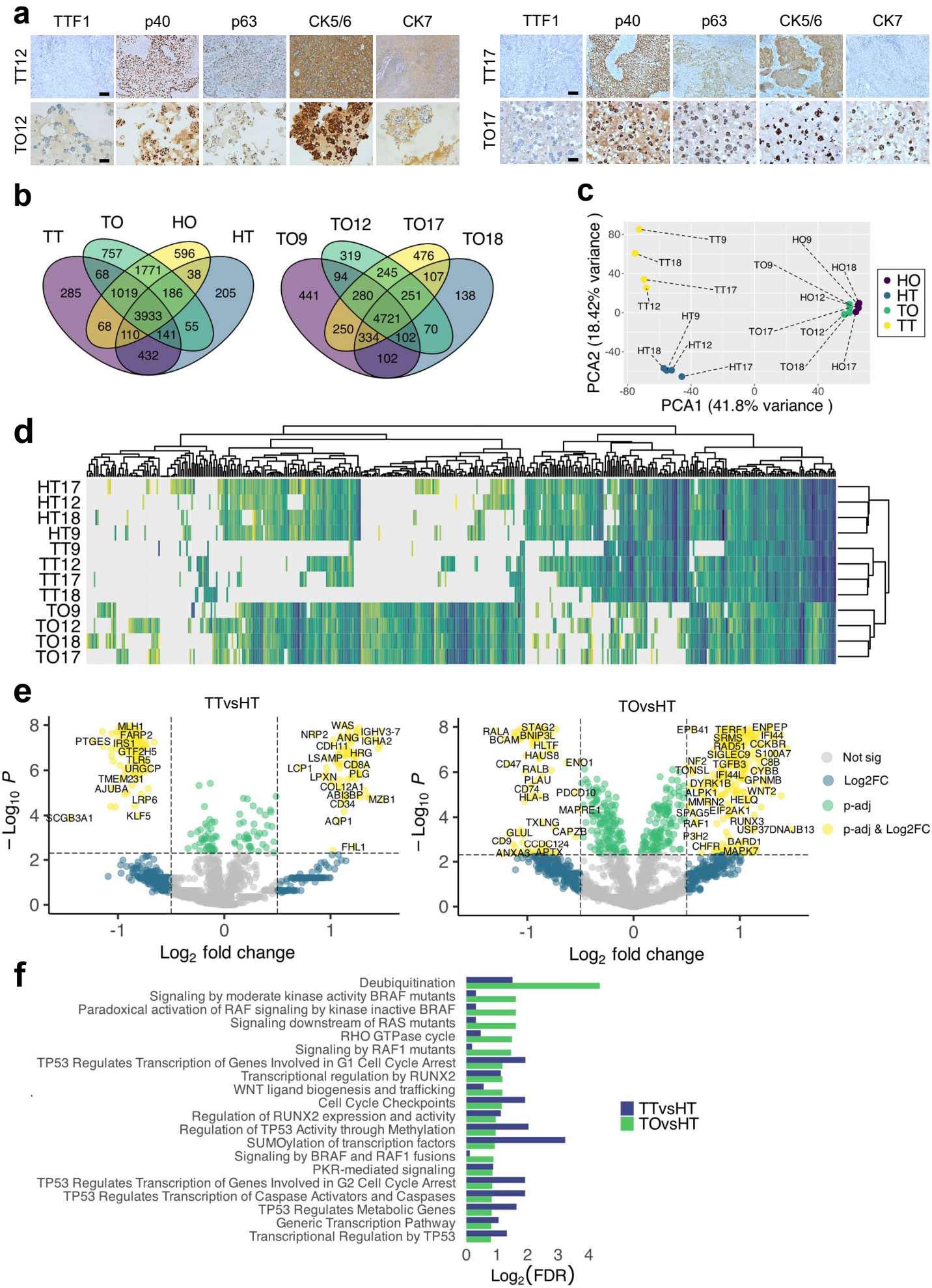

Extended Data Figure 2. Continuation of Lung tumoroids preserve the histological and proteome landscape of their parental tumors and enable individualized proteome profiling. a, IHC staining for lung cancer-associated markers. Positive antibody staining is shown in brown, with hematoxylin counterstaining in blue. TTF1-, p40+, p63+, CK5/6+ and CK7+ (TT12/TO12) / CK7- (TT17/TO17) staining in squamous cell carcinoma primary samples (TT) and matched tumoroids (TO) of patient 12 and patient 17. Scale bars, 100 µm. **b**, Venn diagrams showing protein distributions of TT, TO, healthy organoids (HO) and healthy primary tissues (HT) (left) and protein distributions of TO. Numbers indicate the number of detected proteins. **c**, Principal component analysis (PCA) showing HO, HT, TO, TT. The percentage of variance explained by PCA1 and PCA2 is indicated. **d**, Heatmap of log2 protein intensities from the NSCLC Protein Atlas gene subset. Maximum distance clustering and ward.D linkage were applied. **e**, Volcano plots showing differential protein expression between TT vs. HT (left) and TO vs. HT (right) using the Cancer Hallmark gene subset (n = 2311 genes). Thresholds: 0.5 log2 fold change and adjusted P value of 0.005. Log2 fold change (x axis) and -log10 of adjusted P value are shown (y axis). **f**, Bar plot displaying the log2 false discovery rate (FDR) of selected pathways associated with the TOP20 mutations, as identified through targeted DNA sequencing.

Extended Data Fig.3: Overgrowth of tumoroid cultures by healthy cells as detected by immunohistochemistry (IHC)

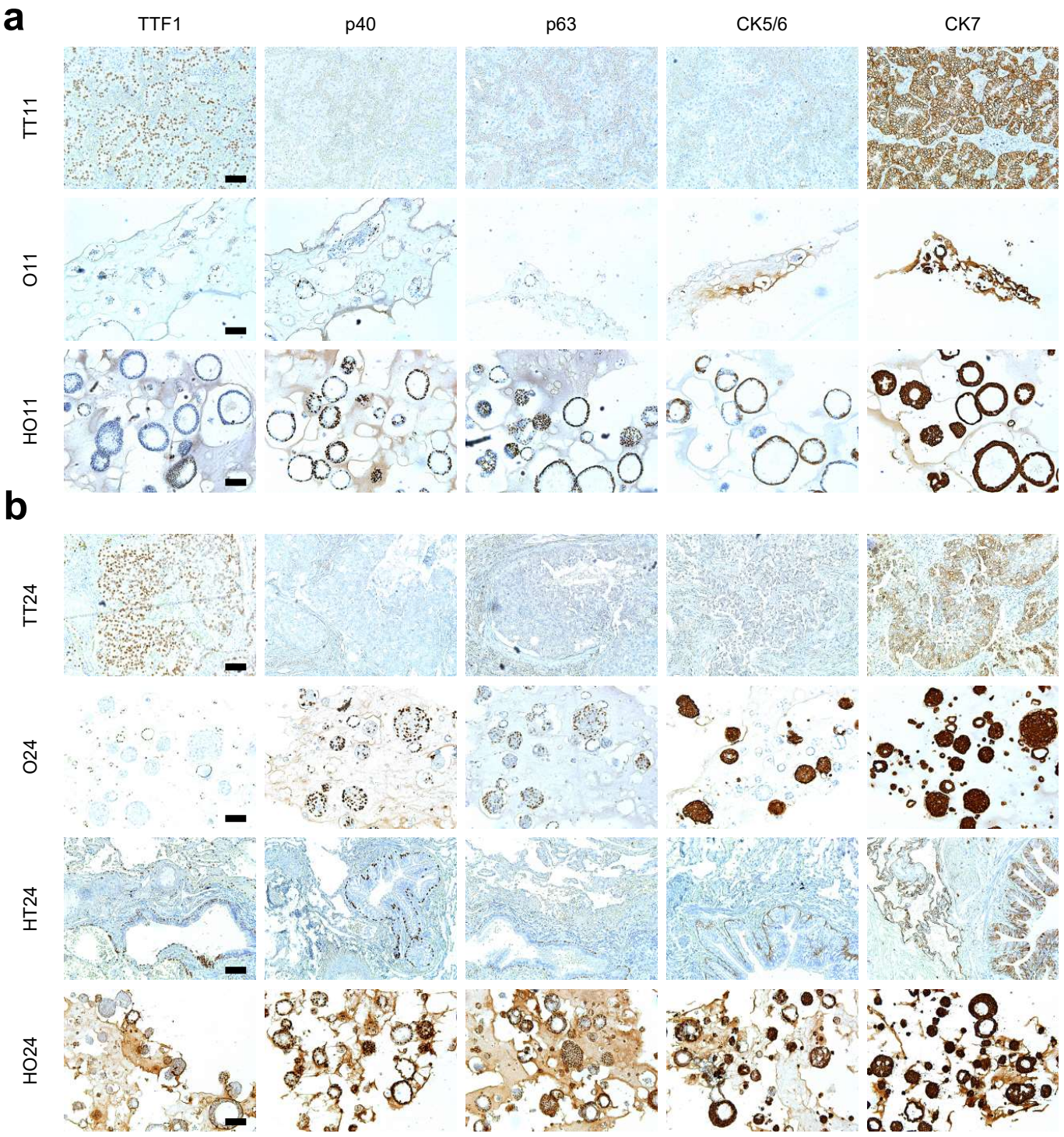

Extended Data Figure 3. Immunohistochemical (IHC) analysis of lung cancer-associated markers in primary tumors and overgrown cultures. a + b, IHC staining for lung cancer-associated markers in adenocarcinoma primary tumor samples (TT11, TT24) and overgrown cultures (O11, O24). Positive antibody staining is shown in brown, with hematoxylin counterstaining of nuclei in blue. In contrast to the primary tumors (TT11, TT24), which show TTF1+, p40-, p63-, CK5/6-, CK7+ patterns, the overgrown cultures (O11, O24) resembled the TTF1 mixed, p40+, p63+, CK5/6+, CK7+ pattern of healthy organoids (HO) and bronchial epithelial cells from healthy tissues (HT, **b**). Scale bars, 100 µm.

Extended Data Fig.4: Patients' clinical courses and responses to therapies.

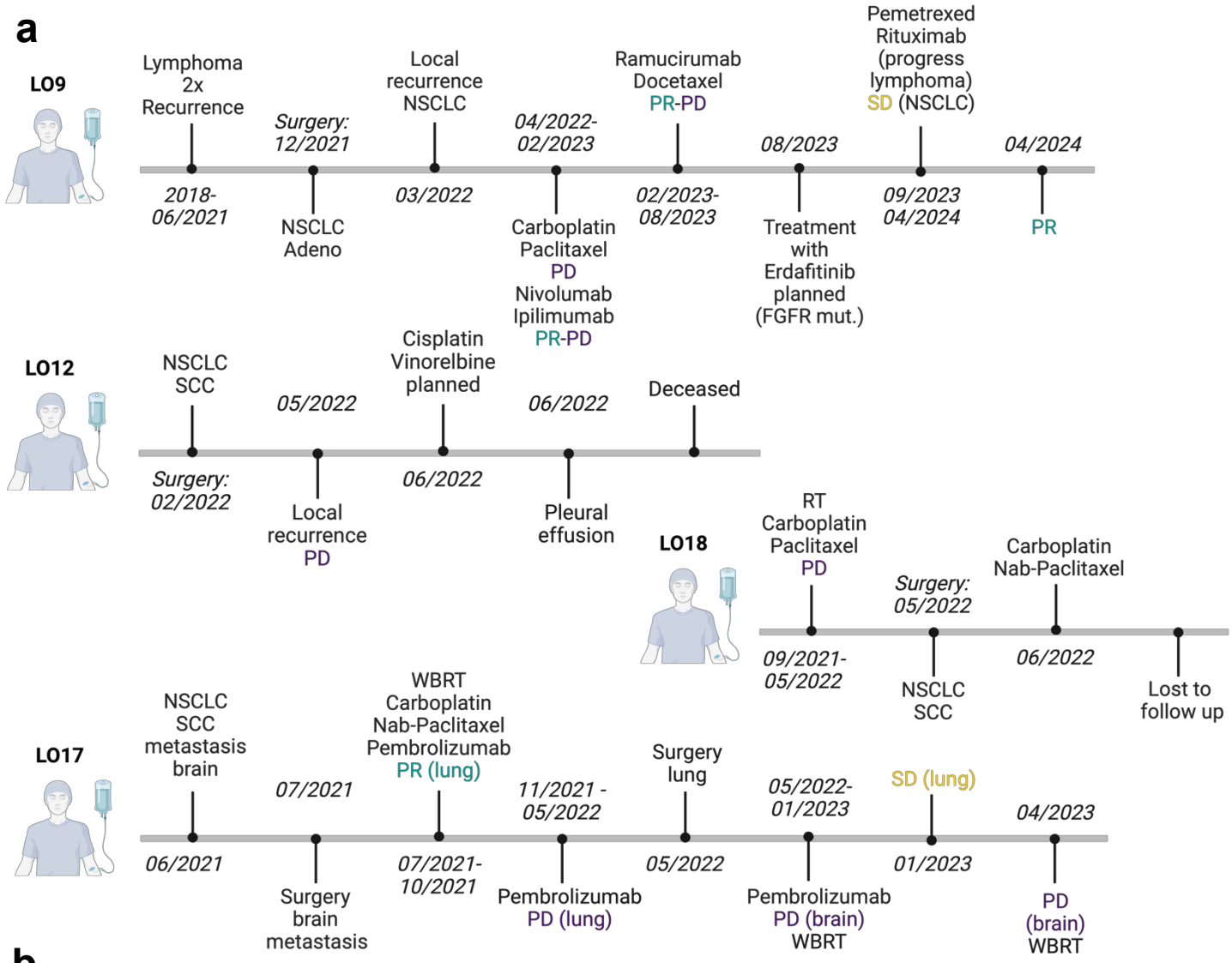

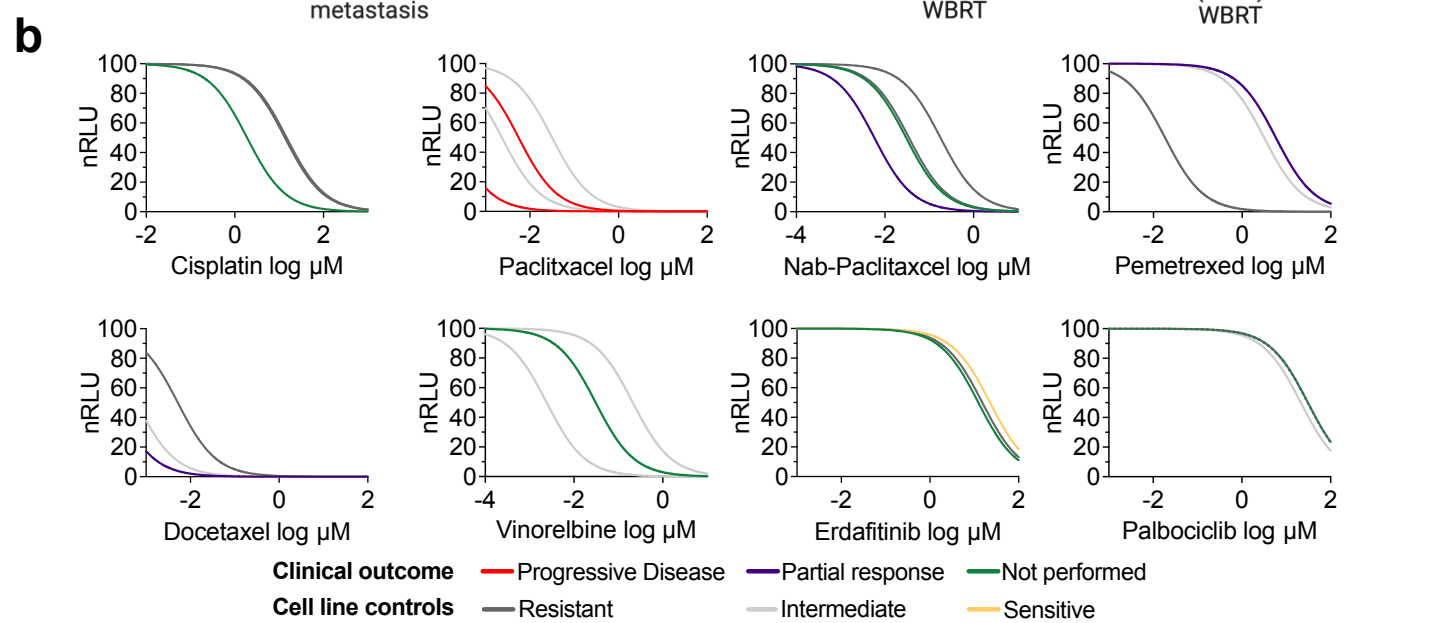

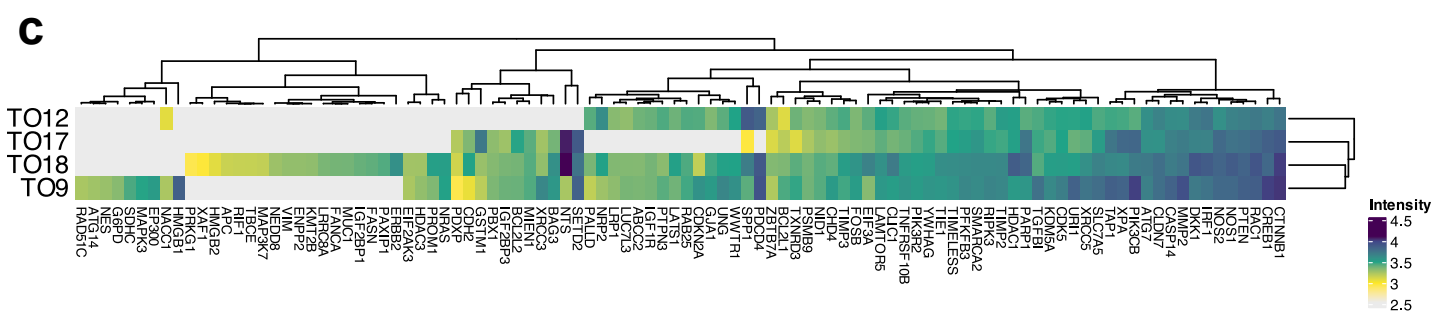

Extended Data Figure 4. Patients' clinical courses and responses to therapies. a, Schematic of clinical courses for patients included in this study. Responses to therapies are classified as progressive disease (PD), partial response (PR), or stable disease (SD) according to RECIST criteria. **b**, Lung cancer cell lines A549 and NCI-H292 were assessed and considered resistant (R), intermediate (I), or sensitive (S) to each chemotherapeutic agent based on CellMiner database. Tumoroids were tested against all chemotherapy regimens administered to patients, corresponding to known clinical outcomes (red for progressive disease; purple for partial response), or for planned therapies where outcomes are unknown (green). **c**, Tumoroid proteomes were filtered to identify proteins linked to resistance to platinum-based chemotherapies. Heatmap showing clustering of resistant tumoroids (TO9 and TO18) and sensitive tumoroids (TO12 and TO17) based on protein intensities, TOP100 proteins with highest ratios of intensity values (TO9/TO18 vs TO12/TO17) are shown.

Extended Data Fig.5: Patients' responses to therapies are retained in matched tumoroids.

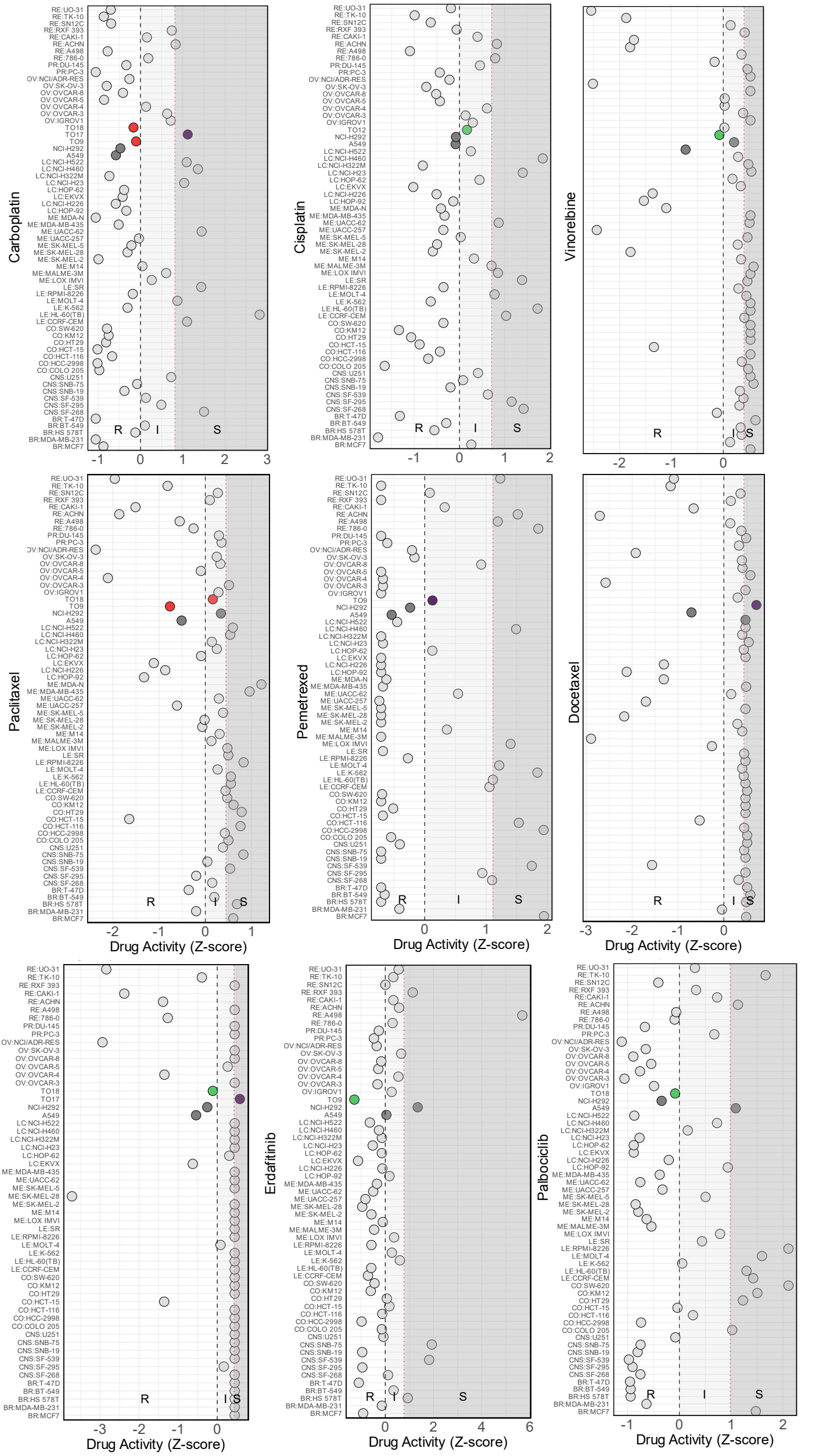

Extended Data Figure 5. Patients' responses to therapies are retained in matched tumoroids. a, Dot plot panels showing drug activity Z-scores (correlating positively with drug sensitivity) from CellMiner database. Based on these scores, cell lines are categorized as resistant (R), intermediate (I), or sensitive (S) to each chemotherapeutic agent. Experimental data from tumoroids (TO) and lung cancer cell lines (A549, NCI-H292, dark grey dots) were aligned with CellMiner database (light grey dots) to infer tumoroid drug sensitivity. For drugs planned in patients' clinical courses where clinical outcome data are unavailable or the drug was not administered, responses were predicted in tumoroids (green circles).

Extended Data Fig.6: Patient's tumor-associated antigen (TAA) screening.

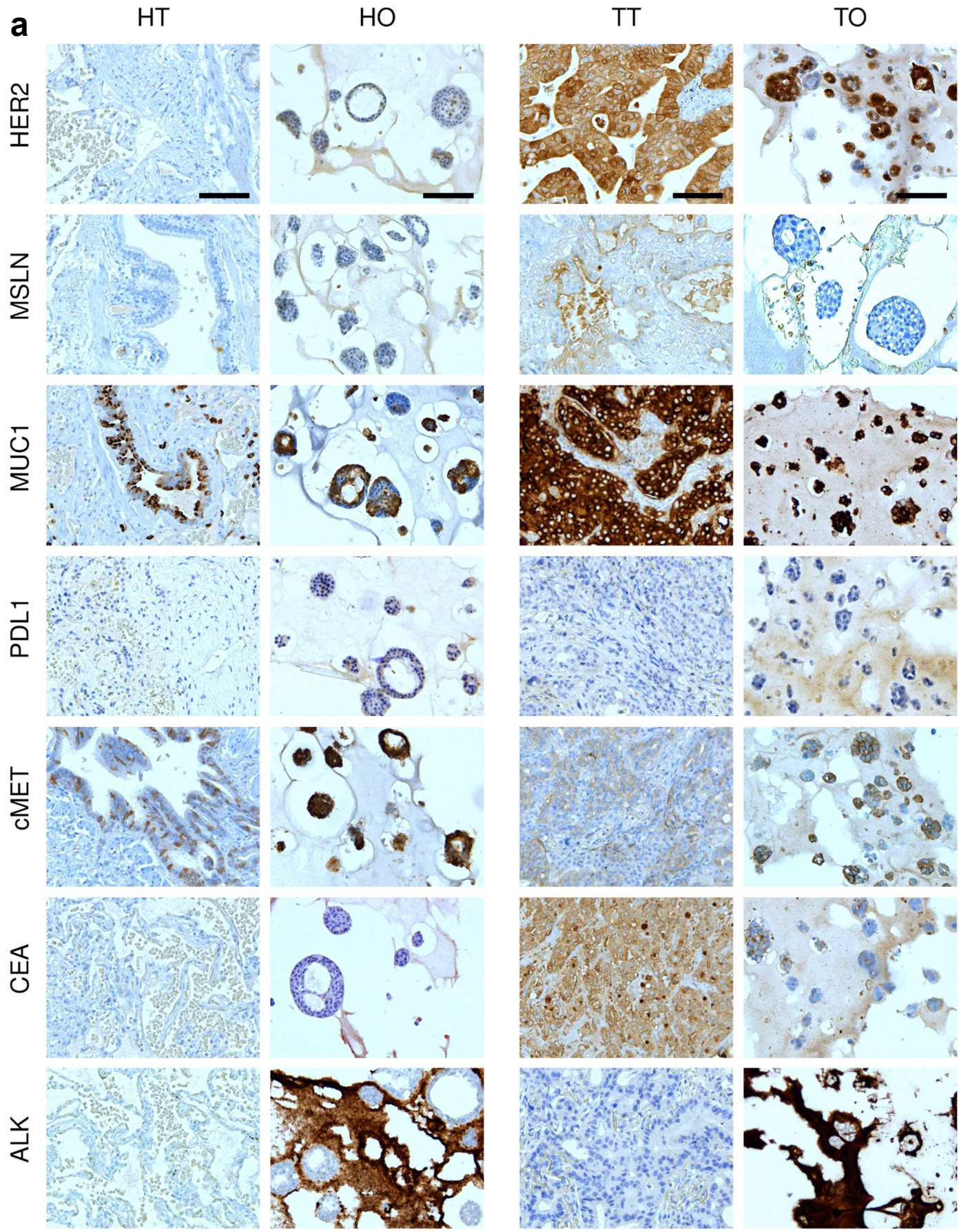

Extended Data Fig.6 (continuation): Patient's tumor-associated antigen (TAA) screening.

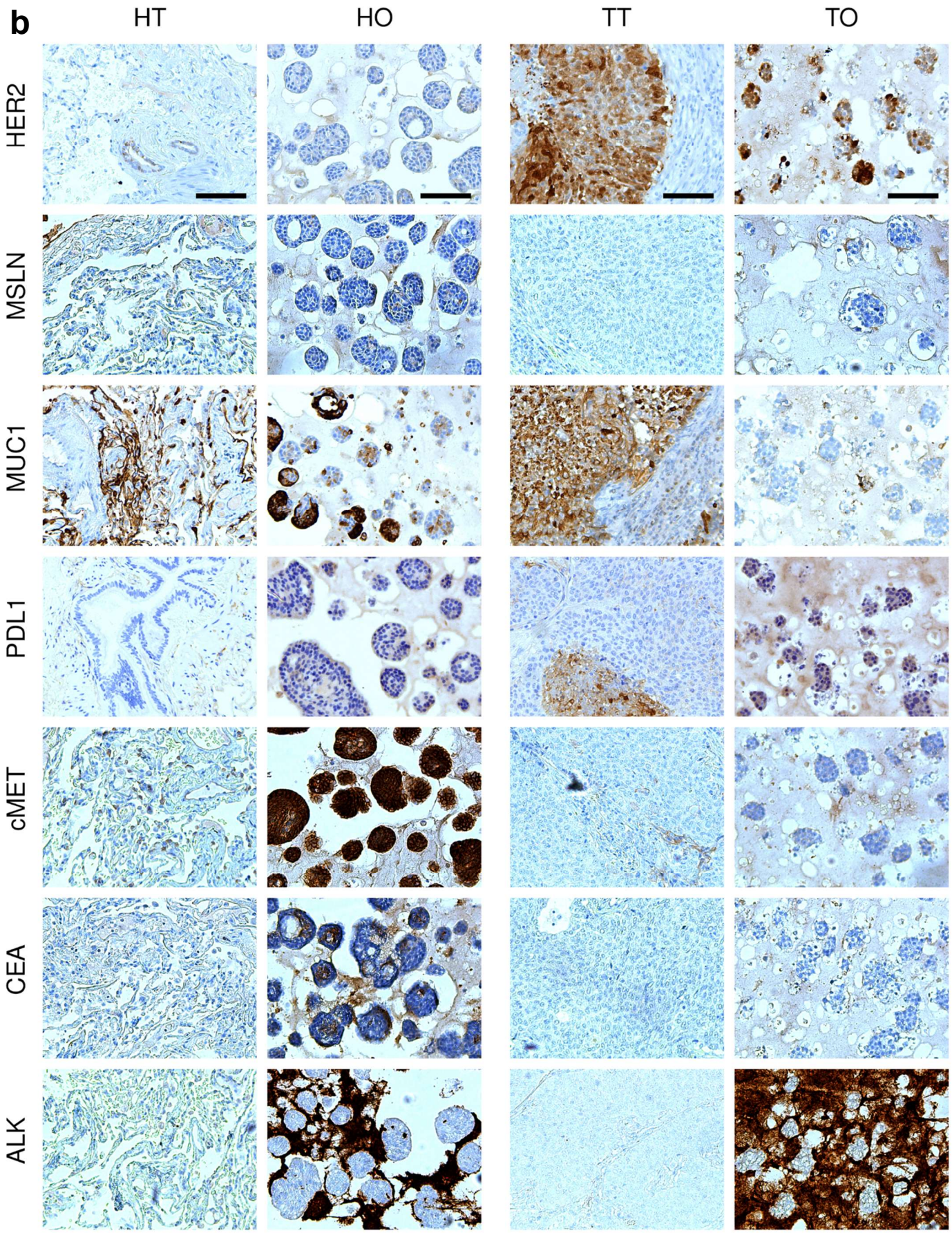

Extended Data Fig.6 (continuation): Patient's tumor-associated antigen (TAA) screening.

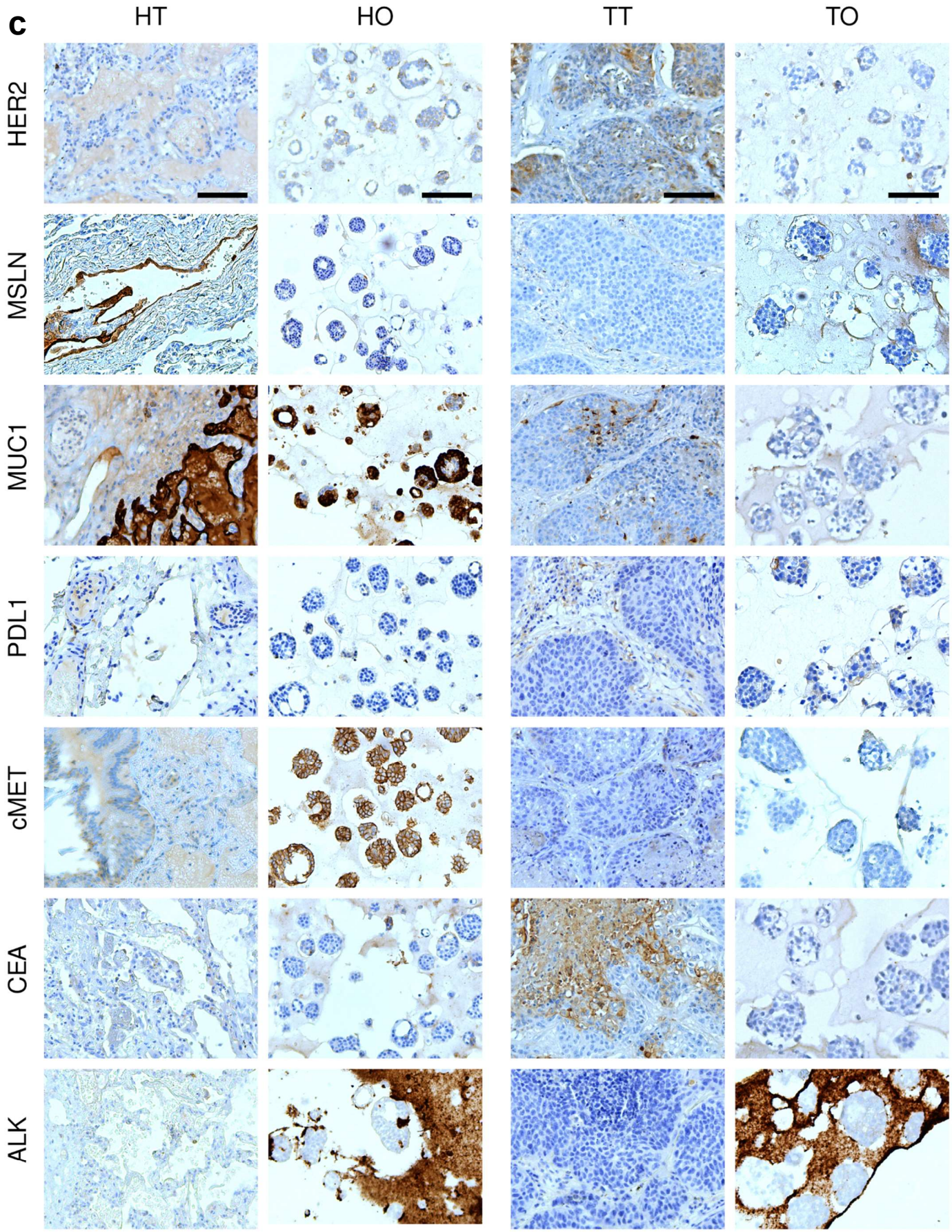

Extended Data Figure 6. Patients' tumor-associated antigen (TAA) screening. Representative images of immunohistochemistry staining for: Erbb2/HER2neu (HER2), Mesothelin (MSLN), Mucin-1 (MUC1), programmed death-ligand 1 (PDL1), hepatocyte growth factor receptor (cMET), carcinoembryonic antigen (CEA), anaplastic lymphoma kinase (ALK) in healthy tissue (HT), healthy organoids (HO), tumor tissue (TT) or tumoroids (TO) are shown for Patient 9 (**a**), Patient 17 (**b**) and Patient 18 (**c**). Scale bars, 100µm.

Extended Data Fig.7: Engineering, gating strategy, and functional assessment of HER2-28z CAR T cells

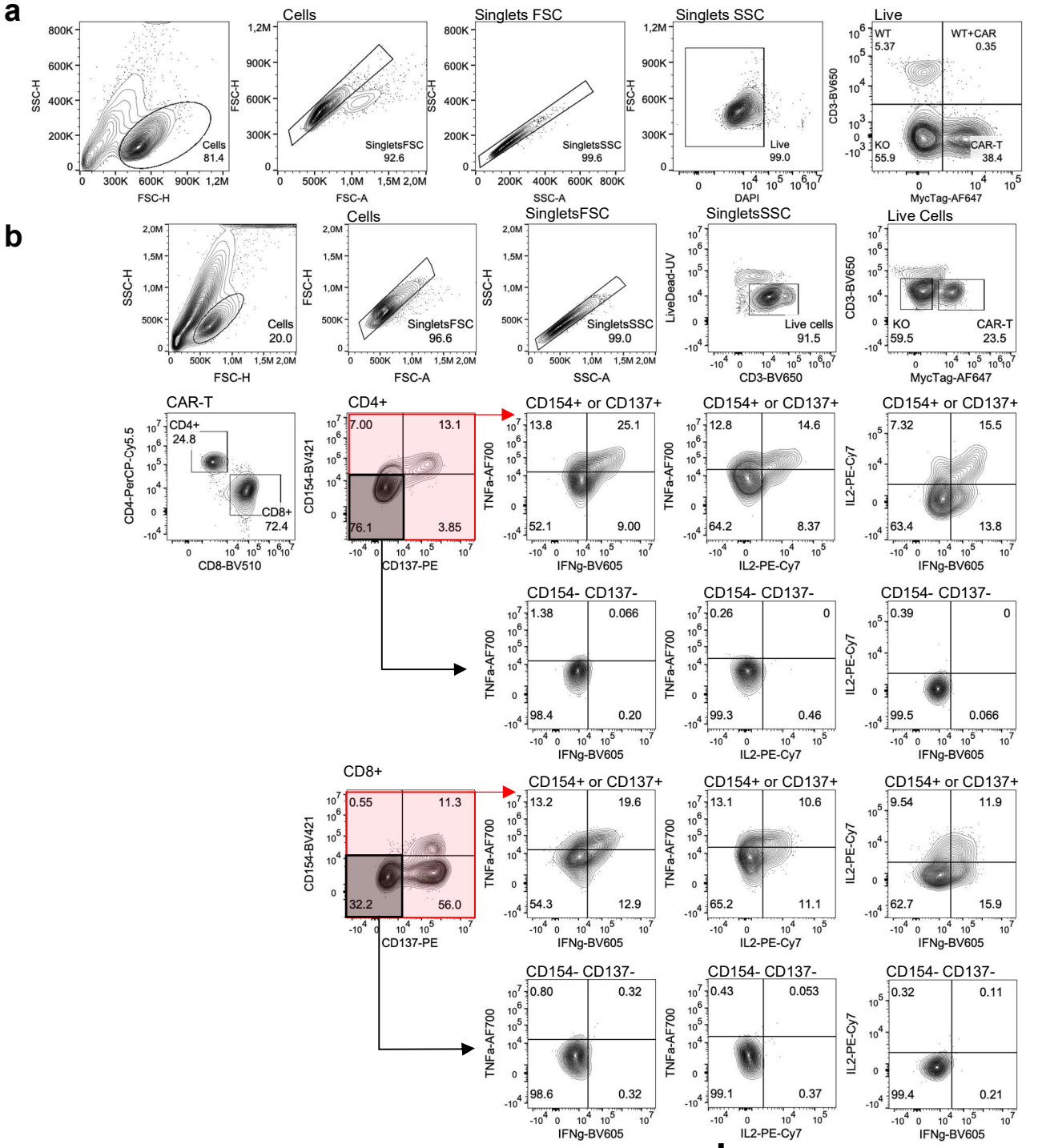

Extended Data Figure 7. Engineering, gating strategy, and functional assessment of HER2-28z CAR T cells. a, T cells from healthy donors are engineered to express a chimeric antigen receptor (CAR) through CRISPR-mediated gene-specific insertion at the *T-cell receptor alpha constant chain* (*TRAC*) locus. MycTag is expressed upstream of the CAR's single chain (scFv) and used to detect CAR T cells. Successfully engineered cells lose the expression of the CD3/TCR complex (KO) and gain the expression of the MycTag (CAR T). CAR T cells are assessed by flow cytometry following the depicted gating strategy. Unedited cells remain wild-type cells (CD3+MycTag-, WT). **b**, Representative gating strategy for HER2-28z CARs stimulated for 16 hours with TO9. **c**, Specific activation of HER2-28z CAR T cells (CD137+ or CD154+) cocultured with HOs was assessed by flow cytometry compared to CD19-28z controls. **d**, Percentage of activated CAR T cells is represented in left Y-axis and cumulative percentages of activated CAR T secreting one, two or three cytokines (IL-2, TNFα, IFNγ) are shown in right Y-axis. *p-value < 0.05 assessed by One-way ANOVA ad hoc Holm-Sidak's multiple comparison test. n = 3 healthy donors in two independent experiments. Mean + standard error of the mean is plotted.

Extended Data Fig. 8: Killing assay setup and imaging analysis

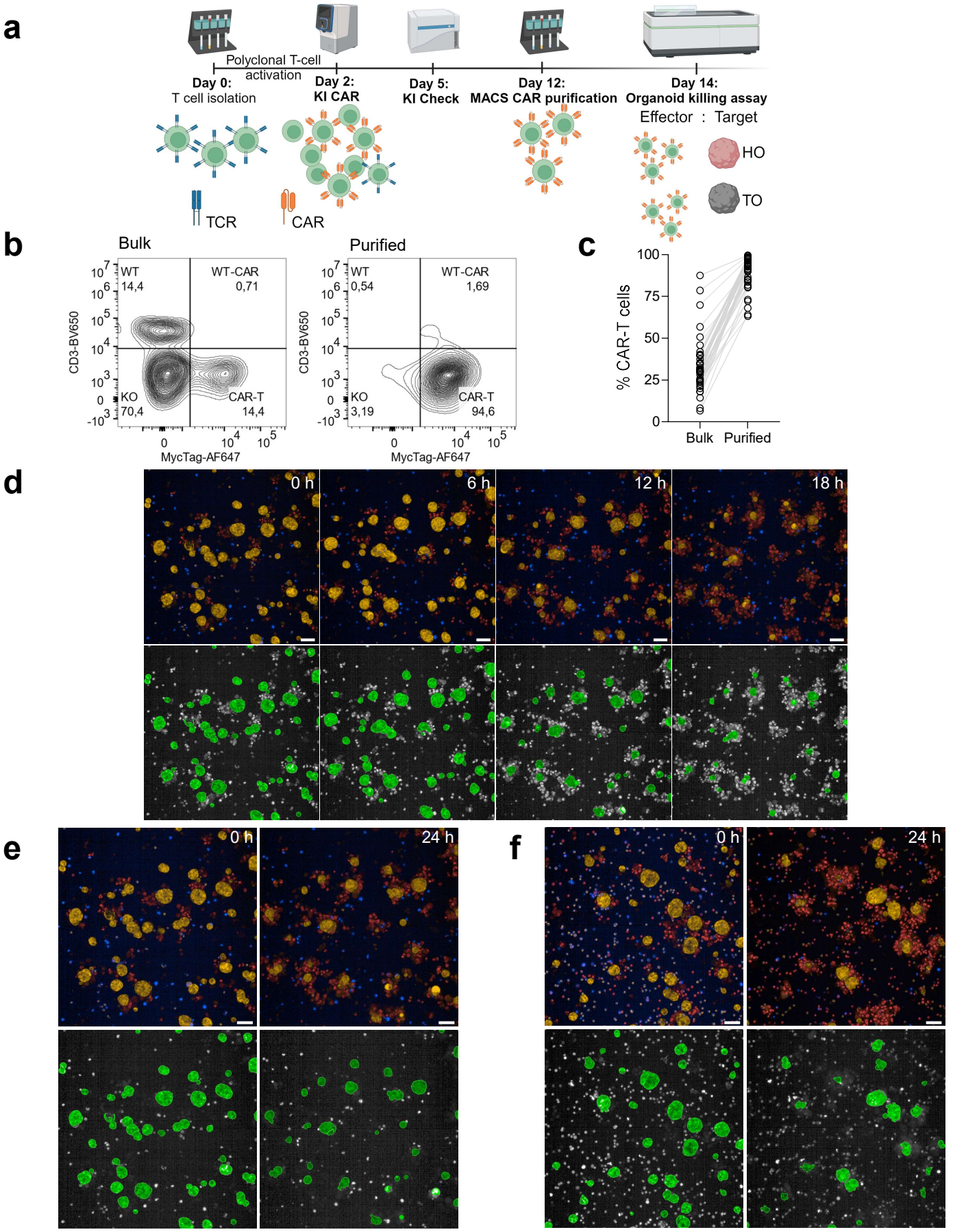

Extended Data Figure 8. Killing assay setup and imaging analysis. a, Representative scheme for bulk or purified CAR T-cell killing assay created with Biorender.com. **b**, Representative contour flow cytometry plot of bulk (left) or purified (right) CAR T cells. **c**, Percentage of CAR T positive cells before (bulk) and after MACS enrichment (purified) linked with a grey line. **d**, Representative images (top: Live cells (yellow), Dead cells (red), CAR T cells (blue)) and corresponding imaging mask (bottom) detecting only intact organoids (green) over time. Scale bars, 50 µm. Exemplary image analysis of tumoroid killing by purified CAR T cells (**e,** top) or bulk (**f**, top) and corresponding masking and detection of intact tumoroids (bottom). Scale bars, 50 µm.

Extended Data Fig.9: Patient-individual CAR T-cell response ex vivo.

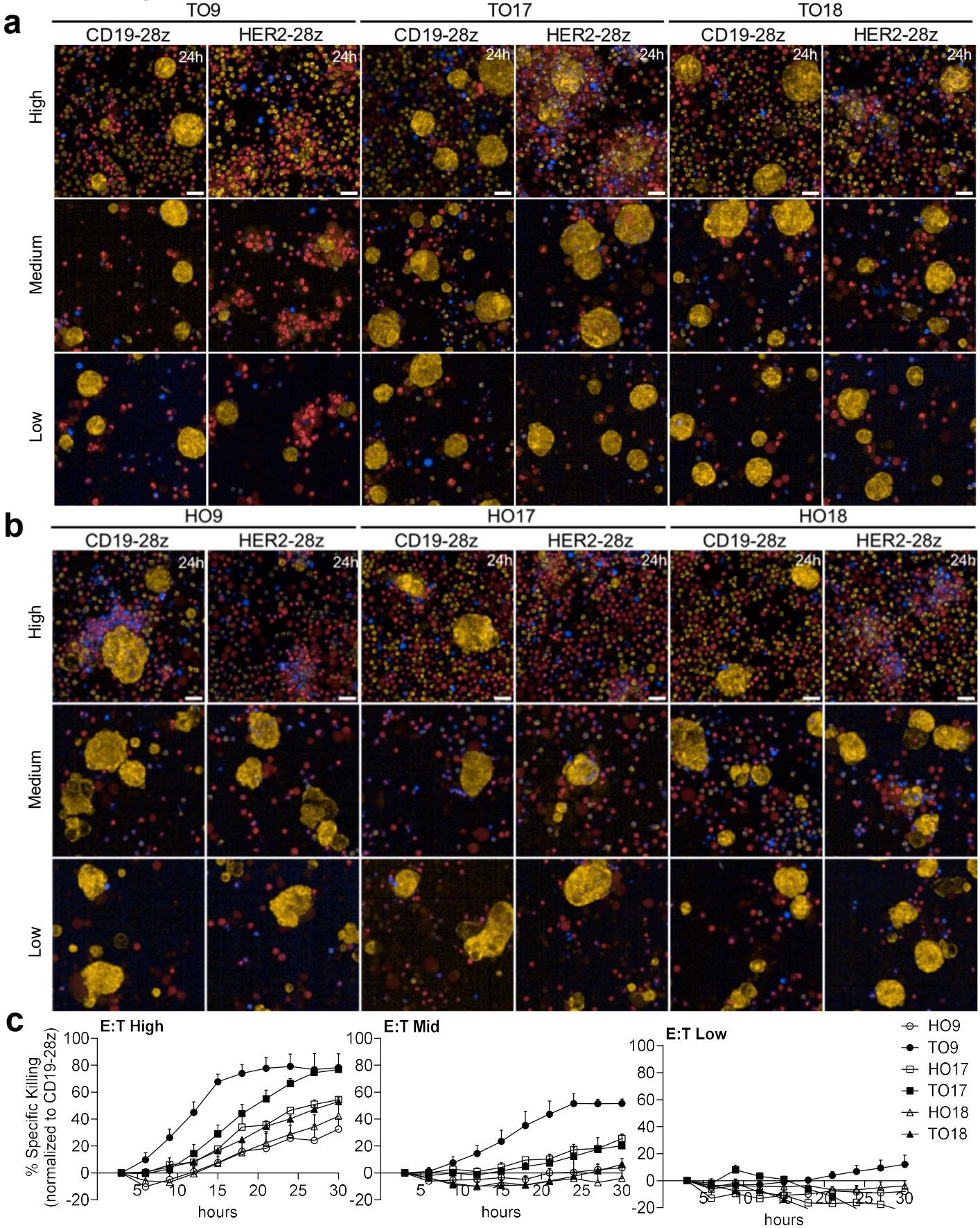

Extended Data Figure 9. Patient-individual CAR T-cell response ex vivo. a + **b**, Representative images of TO (a) and HO (b) killing of HER2-28z CARs compared to control CD19-28z CARs at three different effector to target ratios (High, medium, low). Live organoid cells are stained with NucRed (yellow), dead cells (red), and CAR-T cells pre-stained with efluor 450 (blue). Specific killing is shown by disruption of organoids and staining of NucRed (dead, red). Scale bars, 25 µm. **c,** HER2-28z CAR T-cell killing was normalized by subtracting the irrelevant CD19-28z CAR positive killing and plotted as a percentage of specific killing (Y-axis) over time (X-axis) (see Methods). Mean of 100-150 organoids per experiment with 4 different T-cell donors in two independent experiments is shown + standard error of the mean.

Extended Data Fig.10: CAR T-cell cell activation and resistance mechanisms

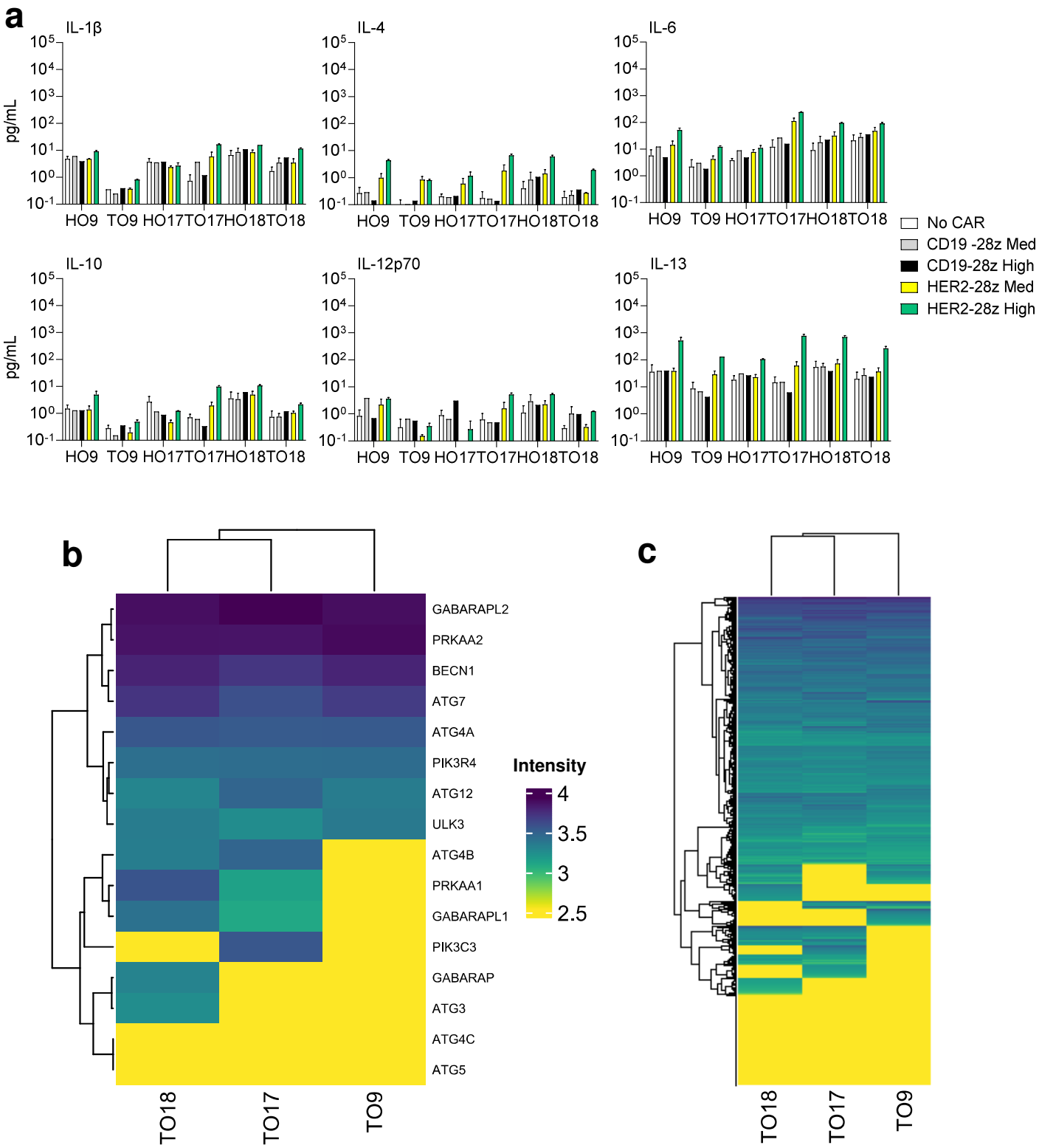

Extended Data Figure 10. CAR T-cell activation and resistance mechanisms. a, Panel of pro-inflammatory cytokines analyzed from killing assay supernatants. n=1-3 independent donors from 2 independent experiments. **b + c**, Heatmap of $\log_2$ protein intensities from TO9, TO17 and TO18 for a subset of autophagy-related genes (**b**; KEGG pathway database. Supplementary Table 5) or immune-evasion related genes (**c**; MolecularSignatures Database, MSigDB. Supplementary Table 5). Maximum distance clustering and ward.D linkage.